An overall study of a Dual Active Bridge for bidirectional DC/DC conversion

Alberto Rodríguez Alonso
Student Member

Javier Sebastian
Member

Diego G. Lamar
Member

Marta M. Hernando
Member

Aitor Vazquez
Student Member

Universidad de Oviedo. Departamento de Ingeniería Eléctrica, Electrónica de Computadores y Sistemas.
Electronic Power Supply Systems Group.
Campus universitario de Viesques s/n. 33204. Gijón, Asturias. SPAIN.
Tel.: +34 985 182 578. Fax: +34 985 182 138. e-mail: rodriguezalberto@uniovi.es

***Abstract* -- The increase demand of an intermediate storage of electrical energy in battery systems, in particular due to the use of renewable energy, has resulted in the need of bidirectional DC/DC power converters with galvanic isolation. Uninterruptible Power Supplies (UPS), battery charging systems, photovoltaic equipment and auxiliary power supplies in traction applications are examples of some fields of application of this kind of converters.**

A Dual Active Bridge (DAB) bidirectional DC/DC converter is a topology with the advantages of decreased number of devices, soft-switching commutations, low cost, and high efficiency. The use of this topology is proposed for applications where the power density, cost, weight, and reliability are critical factors. In the present paper the steady-state analysis of the converter has been carried out, giving some guidelines for the design (considering soft switching limits and the amount of reactive current) and a small-signal model of the topology. Simulations and experimental results are also presented.

***Index Terms*—Dual Active Bridge, bidirectional, battery charging, soft-switching.**

I. INTRODUCTION

Global climate change and depleting fossil fuel reserves are driving society's quest for a sustainable energy infrastructure. The incorporation of renewable energy is limited in many ways due to the variable and intermittent nature of its output. Hence, energy storage systems have to be used to compensate the source variations. A bidirectional converter, usually with galvanic isolation, is generally needed to control the power flow between the energy storage and the load.

The Dual Active Bridge (DAB, see Figure 1) converter originally proposed in [1] and [2] and analyzed in more detail in [3]-[7], is a bidirectional DC/DC converter based on two active bridges interfaced through a high-frequency transformer (with a great influence of its leakage inductance) enabling power flow in both directions in case of active load.

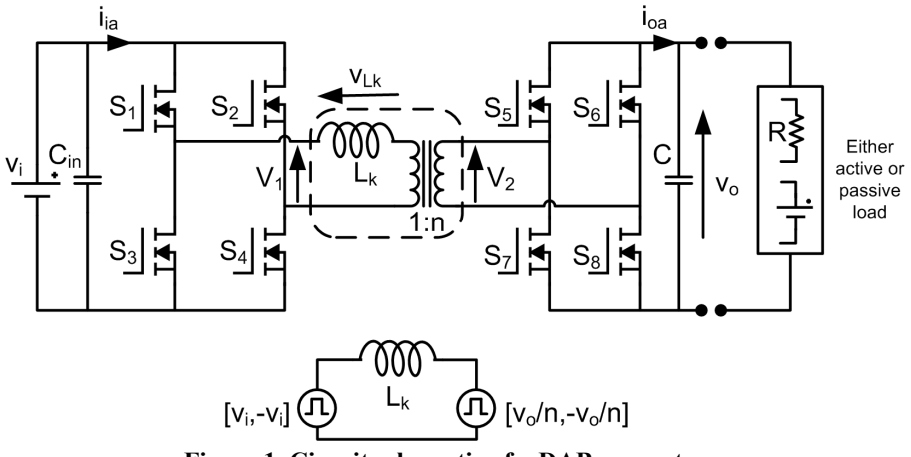

Figure 1. Circuit schematic of a DAB converter

Each bridge is controlled with constant duty cycle (50%) to generate a high-frequency square-wave voltage at its transformer terminals ($\pm v_i$, $\pm v_o$). Considering the presence of the leakage inductance of the transformer, with a controlled and known value, the two square waves can be appropriately phase shifted to control the power flow from one dc-source to the other, so bidirectional power transfer can be achieved. Power is delivered from the bridge which generates the leading square wave.

A complete study of the steady-state and the small signal model are described in the following sections. The basic principles of the DAB converter operating in steady-state will be detailed in the second section. Moreover a subsection will add a design guide, taking into account the limits of the soft switching conditions and the amount of reactive current handled by the converter in different situations. In the third section a simple small signal model of the converter will be presented. In the fourth section some simulation and experimental results will be analyzed to validate the previous models. Finally, in the last section some conclusions are stated.

II. Analysis of the DAB Operating in Steady–State Conditions

The main waveforms of the DAB converter shown in Figure 1 can be seen in Figure 2. All the elements in this study are assumed to have no losses and all the waveforms shown are ideal. The primary bridge is composed by S_1, S_2, S_3 and S_4. The gate signals of S_1 and S_4 are the same. The gate signals of S_2 and S_3 are also identical. The gate signals of S_1 and S_2 are complementary 50% duty cycle signals. With this control signals, the voltage V_1, with values $\pm v_i$, is generated in the primary side of the transformer.

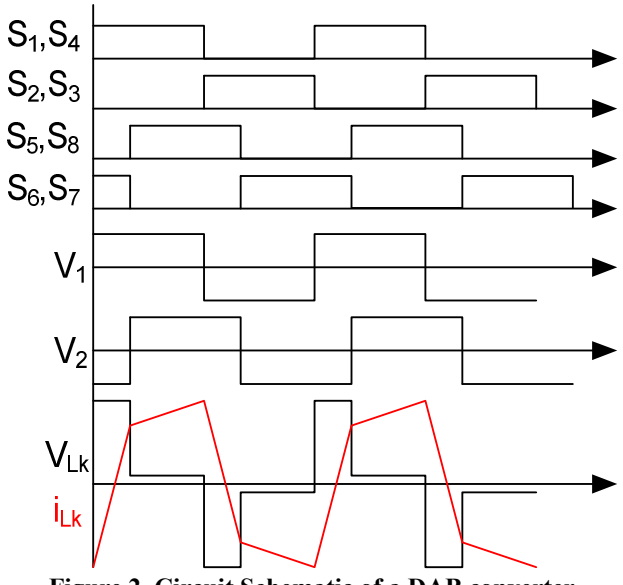

Figure 2. Circuit Schematic of a DAB converter

In a similar way, a voltage V_2 (with values $\pm v_o$) is generated in the secondary side of the transformer, by controlling the switches of the secondary bridge (S_5, S_6, S_7 and S_8). All the control signals of the secondary bridge are similar to the signals of the primary, but with a certain phase shift. These two phase shifted signals (V_1 and V_2) generate a voltage (V_{Lk}) in the leakage inductance (L_k) of the transformer and a certain current flows through it. This current is controlled by the phase shift between the primary and secondary voltages of the transformer.

Once the current through L_k is determined, the input and the output current can be evaluated, as Figure 3 shows. In this figure all the currents are referred to the primary side of the transformer. Due to the symmetry of the circuit, it is only necessary to deduce the equations for a half cycle. Using Faraday's law, and considering the representation of the quantities of the output current in Figure 3(a), equations (1) and (2) are obtained, for the two different states of the converter in a semi-period.

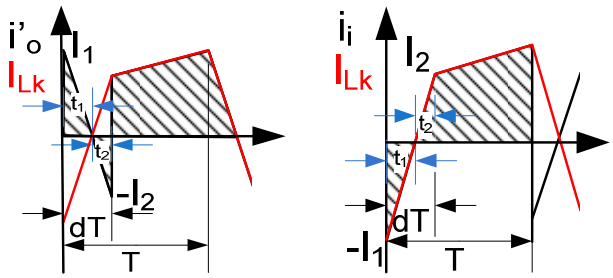

Figure 3. Waveform of the (a) output current and (b) input current

$$\text{For } 0 < t < dT \quad \rightarrow v_i + v_o' = L_k \frac{I_1 + I_2}{dT} \tag{1}$$

$$\text{and for } dT < t < T \quad \rightarrow v_i - v_o' = L_k \frac{I_1 - I_2}{dT} \tag{2},$$

being $V_o' = V_o / n$, $I_1 / t_1 = I_2 / t_2$ and $t_1 + t_2 = dT$.

Solving this set of equations we obtain:

$$I_1 = \frac{T}{2L_k}\left(2v_o' d + v_i + v_o'\right) \tag{3}$$

$$I_2 = \frac{T}{2L_k}\left(2v_i d - v_i + v_o'\right) \tag{4}$$

$$t_1 = T\left(\frac{2v_o' d + v_i - v_o'}{2(v_o' + v_i)}\right) \tag{5}$$

$$t_2 = T\left(\frac{2v_i d + v_o' - v_i}{2(v_o' + v_i)}\right) \tag{6}$$

The average current injected into the output cell (C and load), i_{oa} (Figure 1) is:

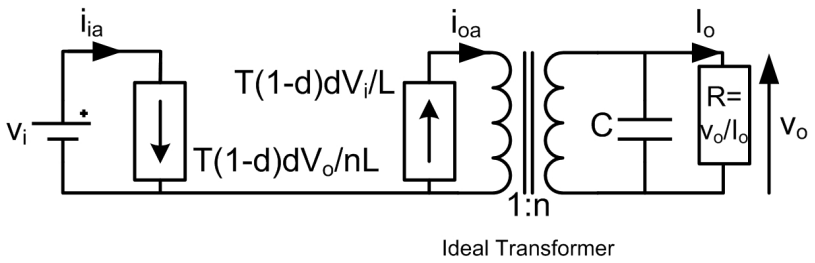

Figure 4. Average model of the DAB converter

$$i_{oa} = \frac{1}{T}\left(\frac{1}{2}I_1 t_1 - \frac{1}{2}I_2 t_2 + (1-d)TI_2 + (1-d)T\frac{1}{2}(I_1 - I_2)\right) \quad (7)$$

From (3), (4), (5) and (6), (7) can be rewritten as,

$$i_{oa} = \frac{(1-d)dTv_i}{L_k} \quad (8)$$

The relation between the input and output voltage can be obtained as,

$$M = \frac{v_o}{nv_i} = \frac{d(1-d)TR}{Ln^2} = d(1-d)k \quad (9)$$

Maximum output voltage is achieved at a duty cycle of 50% as (8) and (9) demonstrate. Using the same analysis than the one used to obtain the average output current, the average input current can be obtained, which expression is shown in equation (10).

$$i_{ia} = \frac{1}{T}\left(\frac{1}{2}I_2 t_2 - \frac{1}{2}I_1 t_1 + (1-d)T\frac{1}{2}(I_1 + I_2)\right) \quad (10)$$

$$i_{ia} = \frac{Td(1-d)v_o}{nL}$$

Finally, with equations (9) and (10) we have the average model shown in Figure 4.

A. Soft switching versus reactive current. Brief design guideline

The constraint which define soft switching conditions (ZVS) can now be specified for the input and the output bridges to be $I_1 > 0$ and $I_2 > 0$ respectively. Equation (11) and (12) give us the limits for the duty cycle to maintain ZVS, being $M=v_o / nv_i$.

$$d > \frac{M-1}{2M}, \text{ if } M \geq 1 \quad (11)$$

$$d > \frac{1-M}{2}, \text{ if } M \leq 1 \quad (12)$$

As Figure 5 shows (green), when M is equal to 1, ZVS is fulfilled for any value of d. Therefore, a good way to design the converter is to select a value of n to have M=1 in nominal conditions. However, when M≠1, ZVS will disappear for light loads. There will be two values of d (for each value of M) which determine the boundaries of ZVS for each bridge ($d_{min,ZVS1}$ and $d_{min,ZVS2}$).

On the other hand, there are reasons for designing the converter using small values of d. One reason is that the evolution of the output current is less lineal for higher values of d, and higher values than 0.35 should be avoided. Another reason is that for higher values of d the reactive current flowing trough the converter will be higher [8]. In equation (13) the sum of the percentage of reactive current at the output and input is evaluated. For M=1, λ_t increases with d, but for M≠1, there are certain values of d to obtain the minimum reactive current. In Figure 5 (red), different curves of constant values of λ_t are represented.

$$\lambda_t = \lambda_o + \lambda_i = \frac{(2d-1+M)^2}{8d(1-d)(1+M)} + \frac{[(2d-1)M+1]^2}{8d(1-d)(1+M)M} \quad (13)$$

In Figure 5 (blue), curves of $M = v_o / nv_i$ for different constant values of $k=TR/n^2L$ (k includes all the design parameters), have also been added.

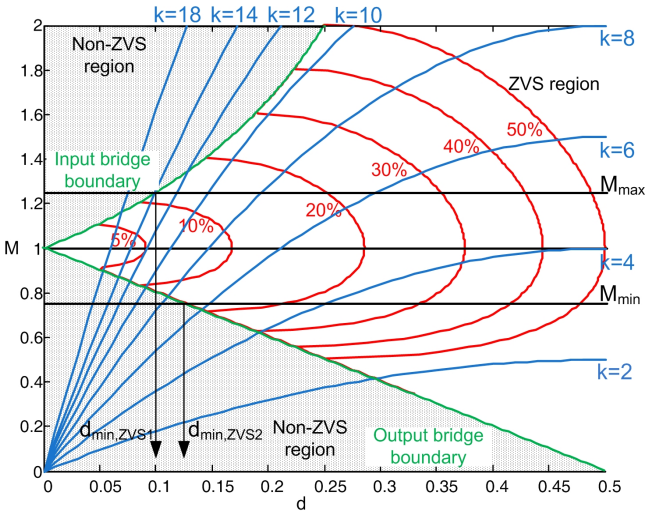

Figure 5. Different quantities to design the converter

Therefore, it is very important to design the converter taking into account that an increase of the value of d will give us greater ranges of ZVS and lower switching losses but high values of reactive current and higher conduction losses. However, for lower values of d, we will be in the opposite situation. For all these reasons the weight of each kind of losses should be evaluated to make a good design.

An example of design is represented in Figure 6. The main

objective has been to obtain a maximum value of reactive current, so the minimum percentage of load to maintain ZVS will be calculated. The design could be obviously done on the other way if maintain ZVS for a wide range of loads was the focus of the application.

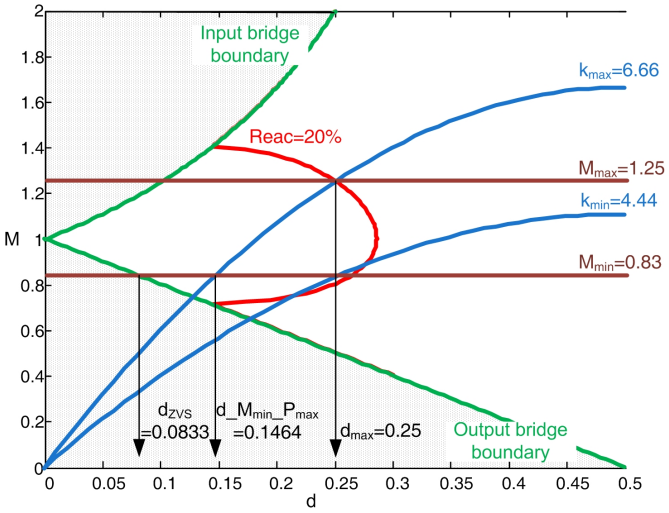

Figure 6. Example of design

The example is done for v_{in}=20V±20%, v_o=200V and a P_{max}=1kW.

- First, the transformer will be designed to have a value of n=10 to obtain M=1 in nominal conditions.
- Second, the minimum and maximum values of M are calculated; in the example, M_{min}=0.83 and M_{max}=1.25.
- Third, the maximum value of λ_t is defined, for example 20%.
- Fourth, the maximum value of d (to maintain λ_t<20%) is calculated for the worst case (minimum of the d_{max} for M_{min} and M_{max}). In the example d_{max}=0.25.
- Fifth, the value of k is calculated from (9); in the example k=6.66. With this value of k we can design the leakage inductance to obtain P_{max} ($Lf=R/n^2k$).
- Sixth, with this design of the converter, the minimum value of load that maintains ZVS can be calculated. The worst case happens with M_{min} and the minimum value of power to achieve ZVS (αP_{max}), so $\alpha=(d_{ZVS}(1-d_{ZVS}))/(d\_M_{min}\_P_{max}(1-d\_M_{min}\_P_{max}))$; in the example α=0.61.

It is important to design the converter looking for the best option to maximize the efficiency. The influence of the switching and conduction losses must be evaluated to know how important is to keep the soft switching conditions to decrease the switching losses. Taking into account that consideration, the increase of the reactive current will imply the increase of the conduction losses.

III. Small-Signal Modelling of the DAB

The small-signal modelling of the DAB converter has been achieved using the well known average techniques described in [9] and [10]. Perturbing equations (8) and (10) of the average output current and the average input current respectively, their small signal model can be obtained. This model is represented by the following equations,

$$\hat{i}_{oa} = \left.\frac{\partial i_{oa}}{\partial d}\right|_0 \hat{d} + \left.\frac{\partial i_{oa}}{\partial v_i}\right|_0 \hat{v}_i = g_{od}\,\hat{d} + g_{ov_i}\,\hat{v}_i \tag{14}$$

$$\hat{i}_{ia} = \left.\frac{\partial i_{ia}}{\partial d}\right|_0 \hat{d} + \left.\frac{\partial i_{ia}}{\partial v_o}\right|_0 \hat{v}_o = g_{id}\,\hat{d} + g_{iv_o}\,\hat{v}_o \tag{15}$$

being,

$$g_{od} = \frac{V_o(1-2D)}{(1-D)DR} \tag{16}$$

$$g_{ov_i} = \frac{V_o}{V_i R} \tag{17}$$

$$g_{id} = \frac{V_o^{\,2}(1-2D)}{V_i(1-D)DR} = \frac{V_o}{V_i}\,g_{od} \tag{18}$$

$$g_{iv_o} = \frac{V_o}{V_i R} \tag{19}$$

From equations (14) and (15) the complete small-signal circuit can be derived, as Figure 7 shows. Finally, equation (20) evaluates the output voltage variations as a function of both the duty cycle and the input voltage variations.

$$\hat{v}_o = \frac{R}{RCs+1}\left(g_{od}\,\hat{d} + g_{ovi}\,\hat{v}_i\right) \tag{20}$$

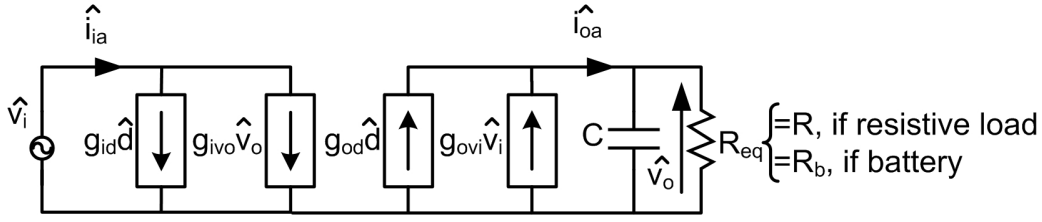

Figure 7. Small signal model

IV. EXPERIMENTAL AND SIMULATION RESULTS

To validate the presented analysis (both steady-state and average small signal) some simulations and a prototype have been developed. First of all, a mathematical spreadsheet in MatLab has been designed to obtain the average currents and the output voltage at steady-state and the small-signal variations predicted by the model in different situations, which can be compared with the simulation results obtained from a circuit working at the switching frequency. The average model has also been simulated, obtaining practically the same results as the mathematical spreadsheet. All the simulations have been carried out by SABER. To experimentally validate all the mathematical expressions and the simulations, a prototype of a DAB has been developed and tested up to 2kW.

Firstly, the steady-state conditions were tested. Some results of the simulation of the converter working at the switching frequency and the ones of the averaged model are shown in Figure 8. In these results only conduction losses in the switches (in the switching frequency simulation) have been taken into account.

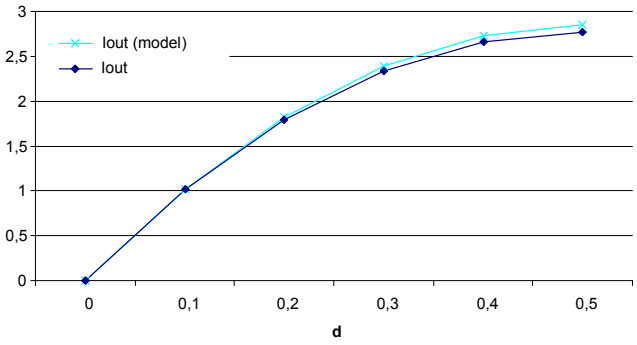

Figure 8. Output current of the model and the switching frequency simulations. V_{in}=20V, R_{out}=134Ω

The basic technical data of the prototype are as follows:

a) Low voltage bridge:
   i) C_{in} = 4.8mF
   ii) Switches: 4 x IRFB4310ZGPBF in parallel
b) High voltage bridge:
   i) C_{out} = 30µF
   ii) Switches: 3 x IPW90R340C3 in parallel
c) Transformer:
   i) Planar E64.
   ii) Turns ratio: n = 1:10.
   iii) Leakage inductance: L_k = 120nH
d) Total DAB converter inductance: L = 1.23µH
e) Switching frequency: f_{sw} = 70kHz

In Figure 9 and Figure 10, the output current for different input voltages and phase shifts of the bridges are respectively shown.

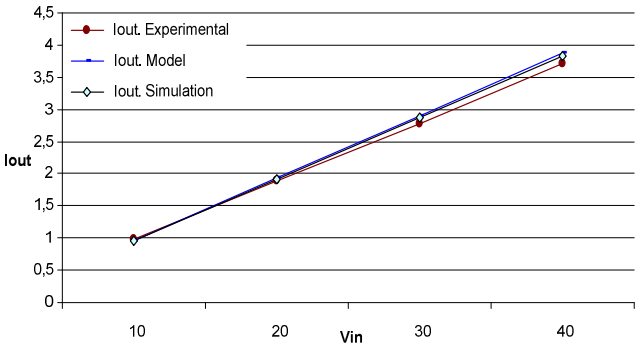

Figure 9. Output current versus input voltage. d = 0.3. R_{out}=134Ω

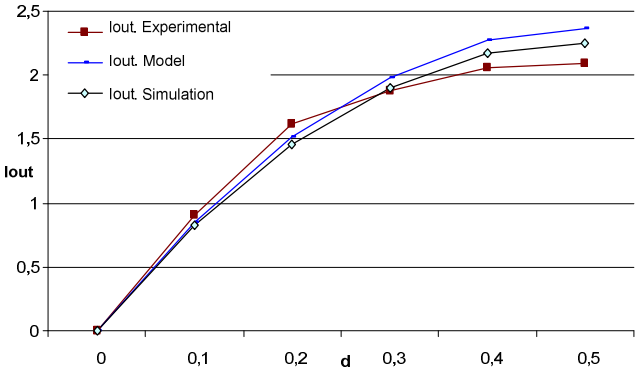

Figure 10. Output current versus phase-shift between the bridges. V_{in}=20V, R_{out}=134Ω

The results of the previous figures (9 and 10) are obtained introducing to the simulated circuits a losses factor to have an efficiency similar to the prototype

Figure 9 and Figure 10 show how the output current predicted by the average model, the simulated and experimental converter are very similar for different values of input voltage and phase shift.

Moreover, the small signal model was tested. Changes in the output voltage will be analyzed for changes in the input voltages (ΔV_{in}=12-10=2V). Firstly, the results obtained by the analytical model (using the spreadsheet), and a simulation of the model without losses have been compared. Figure 11 shows that these results are nearly the same.

The dynamic of the prototype is shown and compared with the simulation results in Figure 12. In these cases some losses have been added to the simulated models (both the switched and the averaged one) to be able to compare better the results with the prototype. The evolution of the output voltage is very similar, following a simple first order response.

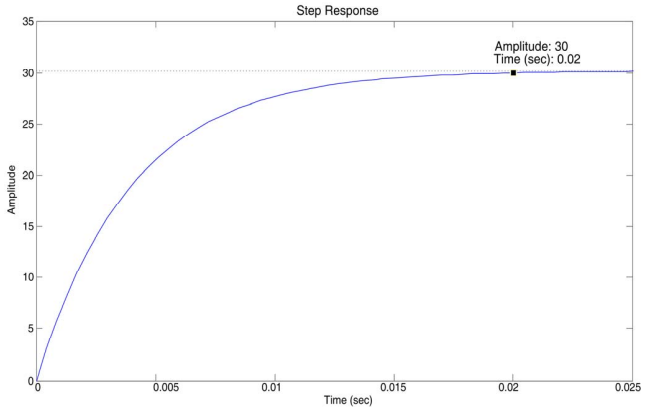

(a)

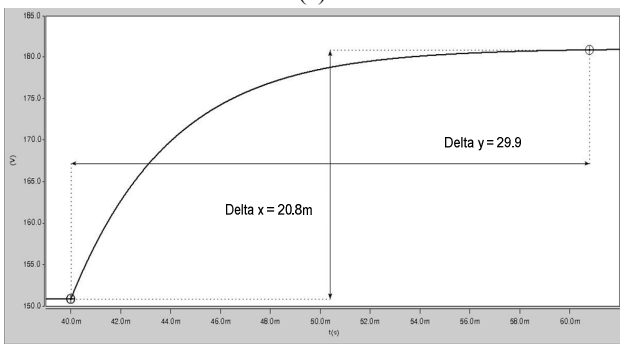

(b)

Figure 11. Step response of the output voltage for a ΔV_{in}=12-10=2V. (a) Analytical model, (b) average model. d= 0.3. Rout=134Ω

The small differences in the variations of amplitude of the output voltage between Figure 11, Figure 12(a) and Figure 12(b) is caused mainly by the different looses existing in the simulation circuits (switched and averaged) and the experimental prototype (however a good time response can be also observed in the experimental results).

V. CONCLUSIONS

A detailed analysis of the steady-state conditions and the small-signal model of the DAB bidirectional converter have been developed and validated with experimental results. Using this model we can predict the steady-state of the converter for different values of parameters such as the switching frequency, input voltage or the phase shift between bridges. The study of the small-signal model predicts a simple first-order dynamics, which allows us to develop an appropriate control for the converter. Moreover, as the circuit has not any reactive element able to keep electric energy for various operation periods, it can be predicted that variations in the input power are instantaneously present in the output power.

Some design guidelines are introduced to obtain the desired values of reactive current and ranges of soft switching conditions.

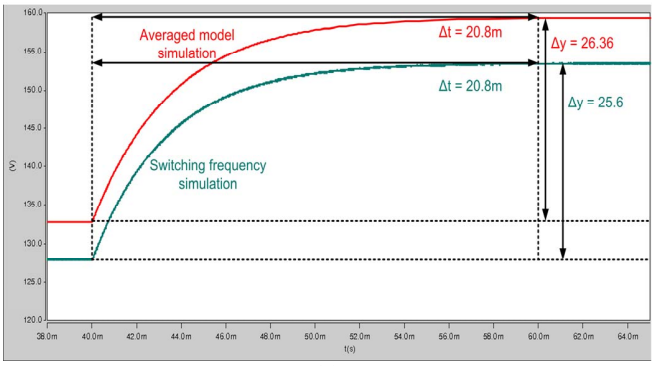

(a)

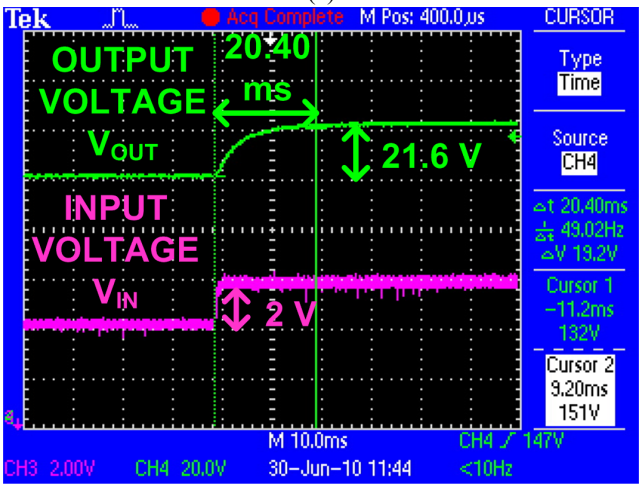

(b)

Figure 12. Step response of the output voltage for a ΔV_{in}=12-10=2V. (a) Simulation circuits with losses and (b) experimental prototype. d= 0.3. Rout=134Ω

To conclude, the DAB converter seems to be a good topology for high power DC/DC bidirectional conversion thanks to the low component stresses, small filter components, low switching losses and simple first-order dynamics.

ACKNOWLEDGMENT

This work was supported by the Spanish Ministry of Science and Education under Formación de Profesorado Universitario Program AP2008-03380, and funded by the Spanish Government, the Regional Government and the European Union (FEDER funds) under TEC 2007-66917 and IB09-038 projects.

REFERENCES

[1] R. W. DeDoncker, D.M. Divan, M.H. Kheraluwala, "A three-phase soft-switched high power-density dc/dc converter for high –power applications", IEEE Transactions on Industry Applications, Vol. 27, pp. 63-73, January 1991.

[2] M. H. Kheraluwala, R. W. Gascoigne, D. M. Divan and E.D. Baumann, "Performance characterization of a high-power dual active bridge dc-to-dc converter", IEEE Transactions on Industry Applications, vol. 28, pp. 1294-1301, November 1992.

[3] G. D. Demetriades, “On Small-signal analysis and control of the single and the dual active bridge topologies”, PhD. Thesis, KTH, Stockholm, Sweden, 2005.
[4] F. Krismer, J. W. Kolar, “Accurate power loss model derivation of a high-current dual active bridge converter for an automotive application”, IEEE Transactions on Industrial Electronics, vol. 57, no3, March 2010.
[5] Y. Xie, J. Sun, J. S. Freudenberg, “Power flow characterization of a bidirectional galvanically isolated hig-power DC/DC converter over a wide operating range”, IEEE Transactions on Power Electronics, vol. 25, no. 1, January 2010.
[6] F. Krismer, S. Round, and J. W. Kolar, “Performance optimization of a high current dual active bridge with a wide operating voltage range,” in Proc. IEEE PESC, Jun. 2006, pp. 1–7.
[7] F. Krismer, J.W. Kolar, “Accurate small-signal model for the digital control o fan automotive bidirectional dual active bridge”, IEEE transactions on power electronics, vol. 24, no. 12, December 2009.
[8] Hua Bai, Chis Mi, “Eliminate reactive power and increase system efficiency of isolated bidirectional Dual-Active-Bridge DC-DC converters using novel Dual-phase –Shift control”, IEEE Transactions on Power Electronics, Vol.23, No. 6, pp. 2905-2914. November 2008.
[9] R.D. Middlebrook, “A continuous model for the tapped inductor boost converter”, IEEE PESC 1975, p.p. 63-79.
[10] R.D. Middlebrook and Slobodan Cuk, “A general unified approach to modelling switching-converter power stages”, IEEE PESC 1976, p.p. 18-30.